Long-time nonlinear dynamical evolution for P-band ultracold atoms in an optical lattice

Dong Hu,[1] Linxiao Niu,[1] Baoguo Yang,[1] Xuzong Chen,[1] Biao Wu,[2,3,4] Hongwei Xiong,[4] and Xiaoji Zhou[1,*]

[1]*School of Electronics Engineering and Computer Science, Peking University, Beijing 100871, China*

[2]*International Center for Quantum Materials, School of Physics, Peking University, Beijing 100871, China*

[3]*Collaborative Innovation Center of Quantum Matter, Beijing 100871, China*

[4]*Wilczek Quantum Center, College of Science, Zhejiang University of Technology, Hangzhou 310014, China*

(Received 4 June 2015; published 20 October 2015)

We report the long-time nonlinear dynamical evolution of ultracold atomic gases in the P band of an optical lattice. A Bose-Einstein condensate is fast and efficiently loaded into the P band at zero quasimomentum with a nonadiabatic shortcut method. For the first 1.5 ms, this momentum state undergoes oscillations due to coherent superposition of different bands, which are followed by oscillations up to 60 ms of a much longer period. Our analysis shows the dephasing from the nonlinear interaction is very conducive to the long-period oscillations induced by the variable force due to the harmonic confinement.

DOI: 10.1103/PhysRevA.92.043614 PACS number(s): 67.85.−d, 03.75.Hh, 03.75.Lm, 37.10.Jk

I. INTRODUCTION

The occupation of high orbital quantum state in solid-state system is known to play a crucial role to the understanding of a lot of strongly correlated systems, such as high-temperature superconductivity and semiconductor [1]. Ultracold atoms in an optical lattice have been used to simulate quantum many-body systems in the ground state [2]. Recently, there has been increased effort to study ultracold atomic gases in optical lattices at high orbitals [3–5]. This kind of study cannot only help to understand high orbital quantum state in a solid-state system but also provide a chance to study new physics which is completely beyond that of the solid-state system, such as the emergence of the quantum coherence in the first excited Bloch band of an optical lattice [6]. High orbital physics in cold atomic gas has attracted a lot of attention; there are many theoretical predictions, such as supersolids [7] and other novel phases [8–12].

The long-time dynamics of a Bose-Einstein condensate (BEC) in the quantum state of the S band has been intensively studied and many interesting phenomena, such as coherent oscillations [13,14] and nonlinear self-trapping [15,16] were observed. The dynamics of BEC have also been studied in a double-well potential [17]. However, it is much more challenging to observe the long-time dynamics of a BEC in high orbitals because of the difficulty in preparing the cold atoms in such states and maintaining their quantum coherence. For the condensate with a wide quasimomentum distribution in P band [6], the quantum dynamics for the holding time being shorter than 1.3 ms were studied.

Here we experimentally prepare a BEC in the P band of an optical lattice using a nonadiabatic shortcut method and study its long-time quantum dynamics. The initial BEC in the P band with finite size at quasimomentum $q = 0$ has a local maximum in energy so that this state is unstable when the harmonic confinement and interatomic interaction are considered. For the first 1.5 ms, the momentum states undergo fast oscillations. After a brief intermediate interval, the BEC starts a different type of oscillations which have a much longer period (∼14.9 ms) and last up to 60 ms. We find that these long-period oscillations are due to the presence of an additional harmonic trap, and the dephasing induced by the nonlinear interaction is greatly helpful for this oscillation behavior. These counterintuitive features and long-time quantum coherence are possible to study the quantum thermalization.

II. PREPARATION OF P-BAND QUANTUM STATE WITH A SHORTCUT METHOD

In our experiment, we first prepare a pure BEC of about 2×10^5 ^{87}Rb atoms in a hybrid trap which is formed by overlapping a single-beam optical dipole trap with wavelength 1064 nm and a quadrapole magnetic trap. The resulting potential has harmonic trapping frequencies $(\omega_x,\omega_y,\omega_z) = 2\pi \times (28,55,65)$ Hz, respectively. Our lattice is produced by a standing wave created by two counterpropagating laser beams with lattice constant $a = \lambda/2 = 426$ nm along the x direction.

We then load the BEC into the P band by applying a series of pulsed optical lattices within tens of microseconds [18–21]. There are many other methods preparing a BEC in the P-band quantum state [6,22–25]; normally the loading time is tens of milliseconds. Our method has the merit of rapid generation of the quantum state in the P band. More importantly, this method allows us to generate the desired P band with very narrow quasimomentum width around $q = 0$, which is crucial to observe the long-time quantum dynamics. Most recently, this method is proposed to study anisotropic two-dimensional Bose gas [26].

We use two acousto-optic modulators to form our designed pulse sequences with the frequency difference $\delta\omega = 182.5$ MHz which corresponds to a phase shift between two pulse series by $3\pi/4$. This phase shift is crucial to change the parity of the ground state and thus prepare the state in the P band. Four special pulses with a chosen depth V_0 are used to prepare the state in the P band around $q = 0$.

The Hamiltonian of a single atom in a one-dimensional optical lattice can be expressed as

$$H_x = p_x^2/2m + V_0 \cos^2(kx), \tag{1}$$

where V_0 is the depth of the optical lattice, which is in units of E_r, $E_r = (\hbar k)^2/2m$ is the recoil energy of the atom, p_x

*xjzhou@pku.edu.cn

 ©2015 American Physical Society

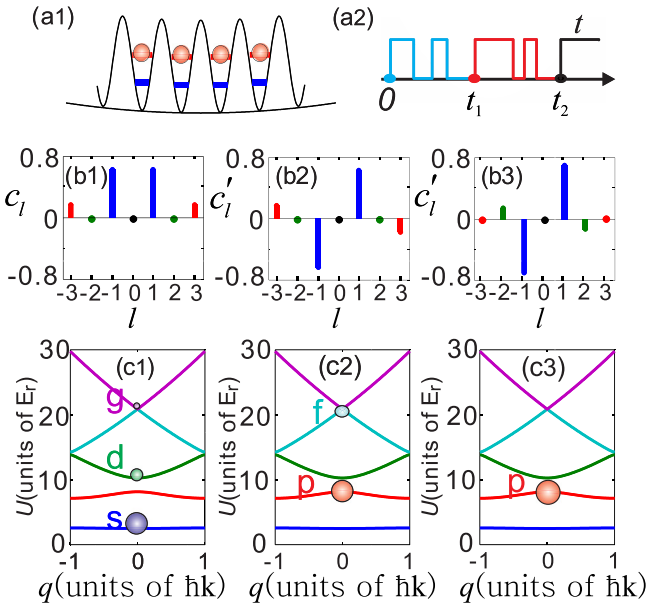

FIG. 1. (Color online) Shortcut loading process of the atoms into P band in 1D optical lattice. (a1) The schematic diagram of atoms in P band. (a2) Loading time sequences with a different phase between the first series of pulses from 0 to t_1 and the second from t_1 to t_2. t is the holding time in the optical lattice. (b1)–(b3) The superposition coefficient c_l right before t_1 and c_l' at the moment right after t_1 and at t_2, respectively. (c1)–(c3) The corresponding population distribution in the Bloch band.

is the momentum of the atom along x direction, m is the atom mass, $k = \pi/a$ is the wave vector, and a is the lattice constant. The eigenstates of the Hamiltonian Eq. (1) are the Bloch states $|n,q\rangle$.

Since the system is periodic, and our loading method conserves the quasimomentum, we can choose the plane waves $|2l\hbar k + q\rangle$ with quasimomentum q as a set of complete bases, i.e.,

$$|\psi\rangle = \sum_l c_l |2l\hbar k + q\rangle, \tag{2}$$

where c_l is the superposition coefficient, $l = 0, \pm1, \pm2, \ldots$ is an index number, $q \in [-k,k)$ is the quasimomentum, and $|2l\hbar k + q\rangle \equiv e^{i(2lk+q/\hbar)x}/\sqrt{2\pi}$ is the eigenstate of p_x. On the other hand, the state $|\psi\rangle$ can also be expressed in the Bloch state $|n,q\rangle$ as $|\psi\rangle = \sum_n \langle n,q|\psi\rangle |n,q\rangle$, where $n = s,p,d,\ldots$ is the band index. The aim state $|\psi_a\rangle$ is the first excited state at $q = 0$, as shown in Fig. 1(a1).

Our shortcut method includes a series of designed standing-wave pulses. The atom state $|\psi\rangle = \prod_{j=1}^{4} U_{f_j}(t_{f_j}) \cdot U_{p_j}(t_{p_j}) \cdot |\psi_0\rangle$, where $U_{p_j}(t_{p_j})$ and $U_{f_j}(t_{f_j})$ are the time evolution operator and free evolution operator for the jth pulse with duration t_{p_j} and t_{f_j}, respectively. The atom experiences spatial period potential in the pulse duration, and the different momentum states can gain different phase factors between the interval.

Our preparation process consists of two series of pulses as shown in Fig. 1(a2), where we need optimize the fidelity $|\langle\psi_a|\psi\rangle|^2$ between the aim state $|\psi_a\rangle$ and $|\psi\rangle$ to its maximum by changing the parameters of pulse sequence. In the first series of pulses from 0 to t_1, the atom experiences spatial potential $V_0 \cos^2(x\pi/a)$. For the second series pulses from t_1 to t_2 the atom experiences potential $V_0 \cos^2(x\pi/a + 3\pi/4)$. The coefficients c_l (c_l') and the distribution in the Bloch band are shown in Figs. 1(b) and 1(c), respectively.

For a pure Bloch state or a superposition state with different Bloch state at $q = 0$, the parity can be given as $P = \sum_l |c_l - c_{-l}|^2/4$, where $P = 1$ stands for a state with odd parity and $P = 0$ even.

At time t_1, all the components in the parity P would satisfy $c_l - c_{-l} = 0$, as shown in Fig. 1(b1), and the atom is distributed in the $s,d,g,\ldots$ bands, as in Fig. 1(c1). However, from the view of the second series of pulses, by the lattice shift, the coefficient c_l would be appended with a phase according to l, as $c_l'|l\rangle = c_l e^{i2l(3\pi/4)}|l\rangle$, and the relation between the coefficients become $c_l' - (-1)^l c_{-l}' = 0$. In our loading process, the first series of pulses ensure that coefficient c_l' with even l is zero, and thus the parity of state can be completely changed as shown in Fig. 1(b2). Its energy-band distribution is in the $p,f,\ldots$, as drawn in Fig. 1(c2). At time t_2, as shown in Figs. 1(b3) and 1(c3), with another two pulses conserving the parity, only the P-band state is populated.

For the quantum state in the S band with $q = 0$, the momentum distribution has peaks around $0\hbar k$ and $\pm2\hbar k$ with $k = 2\pi/\lambda$ [19,27]. For the quantum state in the P band with $q = 0$, because its wave function has the odd parity $\psi(-x) = -\psi(x)$, the momentum distribution equals to zero at $0\hbar k$ and has significant peaks at $\pm2\hbar k$, as shown in Fig. 2(a1), where two dominating peaks at $\pm2\hbar k$ are clearly seen.

III. DYNAMICAL EVOLUTION OF THE QUANTUM STATE IN P BAND

To study the dynamical evolution after a BEC is prepared in the quantum state of the P band, we hold the condensate for time t before measuring the momentum distribution of the ultracold atoms after a time of flight (TOF) of 28 ms. The momentum distributions of the BEC at $t = 0$ ms, 2 ms, 5 ms, 7 ms, and 30 ms are shown in the first row of Figs. 2(a1), 2(a2), 2(a3), 2(a4), and 2(a5). An evolution is clearly observed. The corresponding evolution in the Bloch bands is schematically illustrated in the second row. The depth of the optical lattice is $V_0 = 5E_r$ with E_r being the atomic recoil energy.

The momentum distributions are analyzed by computing the normalized atom populations around momentum states $|l\hbar k\rangle$ ($l = 0, -1, -2$) as $W_l(t) = |\langle l\hbar k|\psi(t)\rangle|^2 = N_l(t)/N$. Here N is the total atom number and $N_l(t)$ is the atomic number around $|l\hbar k\rangle$. In the TOF images we choose 95.2 μm as the width to determine the atom number N_l. This is the width of a condensate without any quantum manipulation and after the free expansion of the same TOF. We find W_l's oscillation with time as shown in Figs. 2(b) and 2(c). In Fig. 2(b), there are rapid oscillations in $W_{-2}(t)$ and $W_0(t)$. These rapid oscillations disappear around $t = 1.5$ ms. After a short transition time, a different type of oscillation begins to emerge around $t = 2$ ms. These oscillations can be observed up to 60 ms and have a much longer period of 14.9 ms. We will show how the interaction would affect this long-period oscillation, which was not observed in the previous work [6].

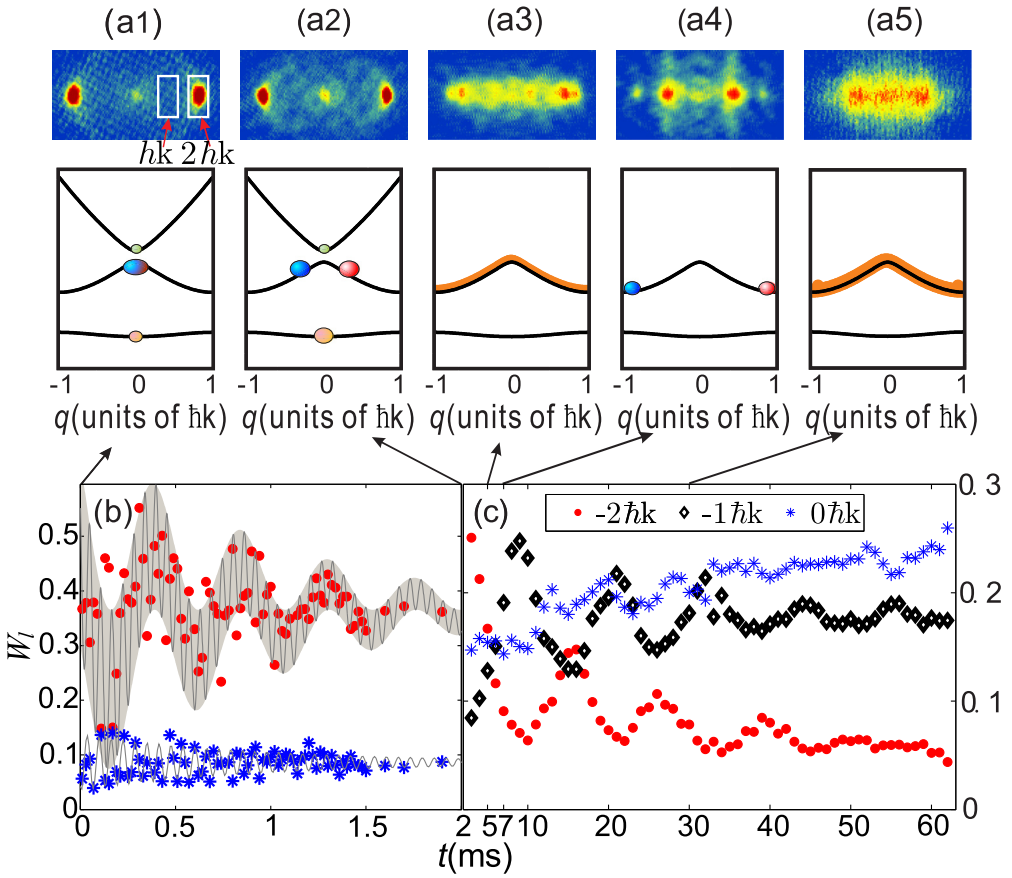

FIG. 2. (Color online) (a1)–(a5) First row: the measured momentum distributions of the BEC in the P band at different holding times (0 ms, 2 ms, 5 ms, 7 ms, and 30 ms), and the white rectangles are region for us to calculate proportion of different momentum states; the second row: schematic illustration of the corresponding population distributions in the Bloch band. (b) Population oscillations around momenta $0\hbar k$ (blue stars) and $-2\hbar k$ (red dots) with $t < 1.5$ ms. Solid lines are from numerical simulations. An oscillating envelope is shown with a shaded region highlighting the slower oscillation component of the rapid oscillations. (c) Population oscillations around momenta $0\hbar k$ (blue stars), $-\hbar k$ (black diamonds), and $-2\hbar k$ (red dots) with $t > 2$ ms. The oscillation period is about 14.9 ms with $V_0 = 5E_r$.

IV. SHORT-PERIOD OSCILLATIONS

The short-period oscillations shown in Fig. 2(b) are beating signal due to coherent superposition of different bands. In real experiment, it is impossible to prepare a quantum state completely in the P band. What we prepared is in fact a superposition of s, p, and d bands with negligible higher band. Due to the difference in time scale of two oscillations and uncertainty in experiment, the experimental data is shown in the figure comparing with the peripheral contour of the beating signal from theoretical simulation with the choice of the initial quantum state $|\psi(t=0)\rangle = \sqrt{0.9}|p,q=0\rangle + \sqrt{0.05}|d,q=0\rangle + \sqrt{0.05}|s,q=0\rangle$.

With this understanding, the periods of the oscillations in Fig. 2(b) are determined by the band gaps. As there are three band gaps between the s, p, and d bands, there should be three oscillating periods, T_{sp}, T_{sd}, and T_{pd}. Around $0\hbar k$, the atoms are mostly from the s and d bands due to the odd parity of the p band. As a result, we expect only one oscillation period T_{sd}. This is indeed what we see for W_0 in Fig. 2(b). Around $-2\hbar k$, all three bands have significant contributions. Because the populations of the s and d bands are both small, the contribution to W_{-2} related to period T_{sd} is of second order and negligible. As a result, only two periods are expected for W_{-2}, T_{sp}, and T_{pd}. For the short-period oscillations of W_{-2}, Fig. 2(b) clearly shows two different oscillation periods, one faster oscillation enveloped by a slower oscillation. This is consistent with the fact that T_{pd} is much larger than T_{sp}. For $V_0 = 5E_r$ we have $T_{sp} = 69.5$ μs and $T_{pd} = 465.5$ μs.

The short-period oscillations in Fig. 2(b) have a slow decay. This decay is mainly due to the decay of population on P band induced by collision between atoms [18], which is already considered in theoretical results in Fig. 2(b) (solid lines). For our system with atomic number 2×10^5 and density of 6.4×10^{13} cm^{-3} for $V_0 = 5E_r$, the calculated decay time is 1.3 ms. It is coincident to the fitting result (1 ms) based on the experimental data, and the decay rate in experiment is larger which can be attributed to other mechanisms including dephasing of the atom cloud. Considering its finite size, the condensate has a narrow quasimomentum distribution around $q = 0$ with a width of $0.06\hbar k$. Our numerical simulation finds that the calculated decay time would increase by about 1.9%, and numerical simulation shows the influence of this distribution to oscillation frequency is also negligible.

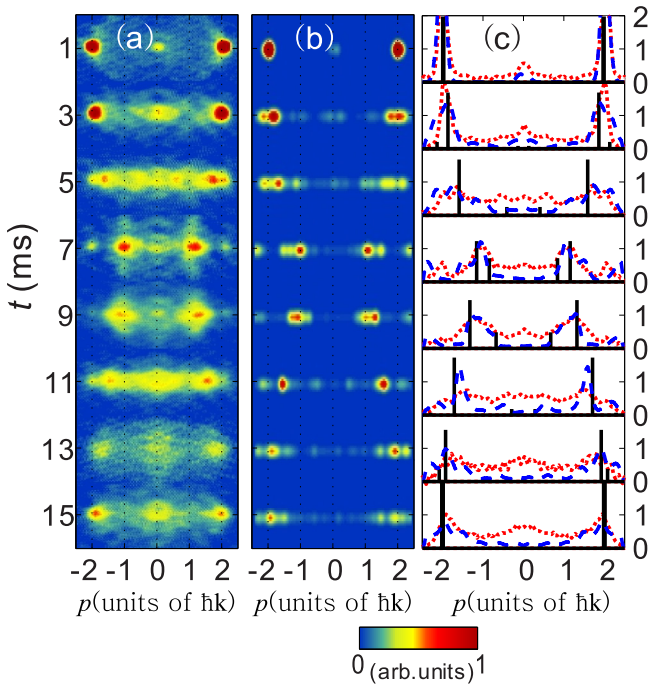

FIG. 3. (Color online) Two-dimensional momentum distributions of the first cycle are shown in (a) and (b) for experiment and theoretical simulation, respectively. After an integration along the vertical direction, (c) gives the one-dimensional distribution for experiment (red dotted line) and numerical simulation (blue dashed line). The black line is obtained from the semiclassical model without considering interatomic interaction.

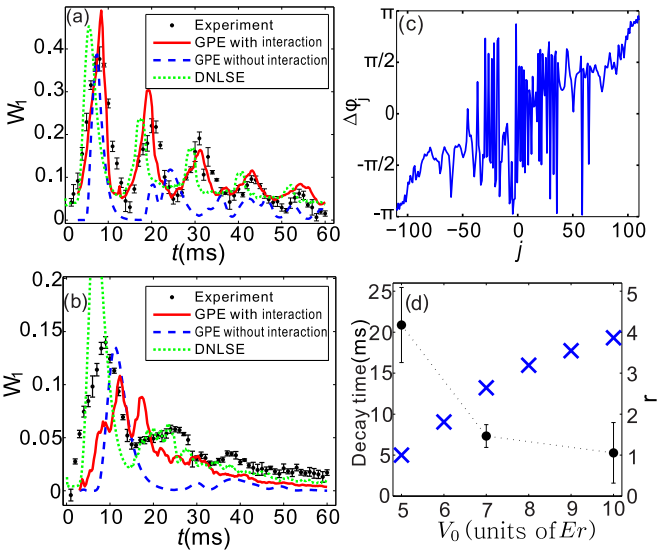

FIG. 4. (Color online) Population with $\hbar k$ vs time t for $5E_r$ (a) and $10E_r$ (b). The experimental results, theoretical simulations with and without the interaction, correspond to the black dots with error bar, red solid curves, and blue dashed curves, respectively, and the green dotted curves are the result of DNLSE. (c) The phase differences between neighboring lattice site j for $V_0 = 5E_r$ and $t = 5$ ms. (d) The dotted points are the measured decay time of the oscillation amplitude, and the cross points are for the dynamical instability ratio.

V. LONG-PERIOD OSCILLATIONS IN THE *P* BAND

The rapid oscillations disappear at about 1.5 ms. After a featureless short dynamical evolution, a different type of oscillation begins to emerge at around 2 ms. As shown in Fig. 2(c), these oscillations have a much longer period of about 15 ms and their oscillating amplitude subsides gradually and becomes zero around 60 ms after five cycles. This is different to the oscillation period of the harmonic trap 35 ms. If we consider this evolution based on the semiclassical model with an effective potential, where the atoms exerted a variable force due to the harmonic trap and quasi-momentum-dependent effective mass, as shown in Appendix A, we see that the period is identical to the experimental result. Different from the Bloch oscillation for atoms on *S* band [14,28,29], however, our analysis shows that these long-period oscillations for atoms on *P* band are greatly affected by the nonlinear dephasing, and this semiclassical model cannot be fully coincident to the experimental observation.

We now look at the experiments in detail. Shown in Fig. 3(a) are the momentum distributions measured experimentally for holding times up to 15 ms, which is roughly the first cycle of the oscillations. At $t = 0$ ms, the momentum mainly distributes around $\pm 2\hbar k$ with $q = 0$, which is the signature of the initial state in the *P* band. At $t = 3$ ms, the absolute value of the peak quasimomentum becomes smaller than $2\hbar k$. This is due to the fact that the kinetic energy is transferred into the potential energy by the harmonic trap. At $t = 5$ ms, the atoms spread to the full regime between $-2\hbar k$ and $+2\hbar k$. At $t = 7$ ms, the atoms concentrate around $\pm\hbar k$, an indication that the quantum state has moved to the Brillouin zone edge of the *P* band [Fig. 2(a4)]. Around 15 ms, most of the atoms have moved back to positions around $\pm 2\hbar k$. Overall, an oscillating pattern is clearly observed in these momentum distributions.

The oscillation pattern can be well captured by our simulation with the Gross-Pitaevskii equation (GPE) as seen in Fig. 3(b), where the simulation is to begin with the ground state in harmonic trap, and carry out with the same experimental process. At the center of the momentum distribution, the experiment shows significant population, which is due to the presence of incoherent atoms. To show it more clearly, we have integrated out the vertical direction and compared the experimental and numerical results in Fig. 3(c). We see that the peak positions are seen clearly matching very well. The experimental results (red dotted line) agree with the theoretical simulation (blue dashed line), where the black line is based on the semiclassical model.

VI. EFFECTS OF THE RANDOM PHASE BETWEEN NEIGHBORING LATTICE SITES ON THE LONG-PERIOD OSCILLATION

The observed time evolution (black dots with error bar) of the proportion with momentum $\hbar k$ is given in Fig. 4(a) for $V_0 = 5E_r$, where we can distinguish five cycles of oscillation. In the figure we have extracted incoherent atoms at the center, and correspondingly the numerical simulation is multiplied by a decay factor. For both $5E_r$ [Fig. 4(a)] and $10E_r$ [Fig. 4(a)], the theoretical simulation with interatomic interaction (red solid curve) agrees with the experimental result, and the agreement between simulation and experiment is better for $5E_r$. It

is quite surprising that the simulation without interatomic interaction (blue dashed curve) doesn't show clear periodic behavior, which differs significantly with the experiment. Both in experiment and theoretical simulation, the interaction has an effect of stabilizing the oscillation. This is counterintuitive by noticing that (i) the repulsive interaction has the effect of widening the wave packet and thus it seems that it should destroy the oscillation; (ii) the interaction usually plays a role of destroying the quantum coherence because of the nonlinear interaction.

To solve this puzzle, we consider the following evolution of the order parameter of the condensate:

$$\Psi(x,t) = \sum_j \sqrt{N_j} \sum_n W_n(x)\psi_{jn}(t). \tag{3}$$

Here N_j is the number of atoms initially in the jth lattice site, while $W_n(x)$ is the Wannier wave function located in the nth lattice site. For atoms in jth site, the initial situation is $\psi_{jn}(0) = \delta_{jn}$. During evolution of the single-site wave function, population would transfer from the jth site to different site n, and $\psi_{jn}(t)$ can be rewritten as $\sqrt{|\psi_{jn}(t)|^2}e^{\phi_{jn}(t)}$. Despite a smooth varying of the external harmonic potential, the contribution of both the kinetic energy and potential energy to the phase $\phi_{jn}(t)$ is the same for every lattice site. However, under tight-binding approximation the time derivative of each site's phase due to the interatomic interaction is proportional to each site's atom number which could be quite different for neighboring lattice sites. As shown in Fig. 4(c), the phase difference between neighboring lattice sites appears completely random because of interatomic interaction at $t = 5$ ms. In a sense, the relative phase between neighboring sites is pseudorandom because it appears random only after the relative phase is confined between $-\pi$ and π.

In this case, when the density distribution or momentum distribution is considered, the interference term between different $\psi_{jn}(t)$ could be omitted, i.e.,

$$\begin{aligned} |\Psi(x,t)|^2 &\approx \sum_j |\psi_j(x,t)|^2 \\ &= \sum_j \sqrt{N_j}\left|\sum_n W_n(x)\psi_{jn}(t)\right|^2. \end{aligned} \tag{4}$$

With the above approximate expression, we solve every $\psi_j(x,t)$ by the discrete nonlinear Schrödinger equation (DNLSE) [13], and then get the momentum distribution, as shown with the green dotted lines in Figs. 4(a) and 4(b). In this situation, our numerical calculations show periodic behavior with each peak shift ahead a little comparing with experiment; however, the period of the time agrees very well with the experimental result. In Appendix B, we give the evolution of the $|\psi_j(x,t)|^2$ which shows that there is long-time period behavior in $|\psi_j(x,t)|^2$. For the condensate in the P band, because in every $\psi_j(x,t)$, it has the peaks around $-2\hbar k$ and $2\hbar k$, the wave packet in every lattice site will split into two parts, propagate in different directions, and oscillate due to the presence of the harmonic trap. It is natural that the incoherent superposition in Eq. (4) will also have the long-time periodic oscillation. For $V_0 = 5E_r$ the GPE agrees better with the experiment than the method of DNLSE and Eq. (4), while here the DNLSE simulation shows the physical picture more clearly. However, for $V_0 = 10E_r$ tunneling between different sites is suppressed, and the incoherent superposition in the DNLSE simulation would be more suitable.

To verify further the role of random phase in the appearance of the long-time period behavior, we add this random phase artificially for the noninteracting case and solve numerically the Schrödinger equation. We find that there is perfect periodic behavior in $W_1(t)$, although the period is a little different from the interaction case.

In Fig. 4(b), we give the experimental result for $V_0 = 10E_r$. We see that the amplitude of the oscillation for $10E_r$ is much smaller than $5E_r$. For $10E_r$, there is a much stronger damping which is due to the highly suppressed tunneling between neighboring sites. In addition, there is no clear periodic behavior in this case. The simulation with GPE doesn't agree well with the experimental result. This may be due to the fact that, at $10E_r$, the particle number is highly squeezed so that there is a breakdown of the mean-field theory, which induces the disappearance of the interference between $\psi_j(x,t)$. Different from the case of $V_0 = 10E_r$, for $5E_r$ the GPE simulation agrees better with the experiment than the method with DNLSE, which shows that at a lattice depth of $5E_r$ coherence between neighboring sites are still maintained.

In the long-time evolution, the oscillation amplitude and damping are greatly affected by the dynamical instability due to the interaction between atoms. When dynamical instability occurs even small perturbations of the wave function would grow exponentially and destroy the state [30,31]. In the following, we calculate the dynamical instability of P band at lattice depth varying from 5 to $10E_r$.

To analyze the dynamical instability, we consider the time-dependent GPE:

$$i\frac{\partial}{\partial\tau}\varphi = -\frac{1}{2}\frac{\partial^2}{\partial x^2}\varphi + \frac{V_0}{16}\cos(x)\varphi + c|\varphi|^2\varphi, \tag{5}$$

with x in units of $1/2k$, τ in units of $m/4\hbar k^2$. $c = \pi n_0 a_s/k^2$ with a_s the s-wave scattering length, n_0 the average density of BEC, and $\sqrt{n_0}$ the units of φ. The nonlinear eigenstates of the time-independent GPE are $\varphi_{n,q}(x) = e^{iqx}\tilde{\varphi}_{n,q}(x)$, where $\tilde{\varphi}_{n,q}(x)$ is periodic with the period of the optical lattice. Considering the deviation,

$$\varphi(x,\tau) = e^{i(qx-\mu\tau)}[\tilde{\varphi}_{n,q}(x) + \delta\tilde{\varphi}_{n,q}(x,\tilde{q},\tau)] \tag{6}$$

and

$$\delta\tilde{\varphi}_{n,q}(x,\tilde{q},\tau) = u_{n,q}(x,\tilde{q},\tau)e^{i\tilde{q}x} + v^*_{n,q}(x,\tilde{q},\tau)e^{-i\tilde{q}x}, \tag{7}$$

with μ the chemical potential and the perturbation momenta $\tilde{q}$ ranging between $-1/2$ and $1/2$. Substituting Eq. (6) and Eq. (7) into Eq. (5) and keeping to the first order, we have

$$i\frac{\partial}{\partial\tau}\begin{pmatrix} u_{n,q} \\ v_{n,q}\end{pmatrix} = \sigma M_{n,q}(\tilde{q})\begin{pmatrix} u_{n,q} \\ v_{n,q}\end{pmatrix}, \tag{8}$$

where

$$\sigma = \begin{pmatrix} I & 0 \\ 0 & -I\end{pmatrix} \tag{9}$$

and

$$M_{n,q}(\tilde{q}) = \begin{pmatrix} \mathcal{L}(q+\tilde{q}) & c\tilde{\varphi}_{n,q}^2 \\ c(\tilde{\varphi}_{n,q}^*)^2 & \mathcal{L}(-q+\tilde{q}) \end{pmatrix}, \tag{10}$$

with $\mathcal{L}(q) = -\frac{1}{2}(\frac{\partial}{\partial x} + iq)^2 + \frac{V_0}{16}\cos(x) - \mu + 2c|\tilde{\varphi}_{n,q}|^2$. The eigenvalues $\varepsilon_q(\tilde{q})$ of the matrix $\sigma M_{n,q}(\tilde{q})$ determine the dynamical stability of the Bloch state $\varphi_{n,q}$. If the imaginary part of $\varepsilon_q(\tilde{q})$ is zero for all $-1/2 \leqslant \tilde{q} \leqslant 1/2$, the state is dynamically stable, otherwise it is dynamically unstable. Here we sum the imaginary part of $\varepsilon_q(\tilde{q})$ for all $-1/2 \leqslant q \leqslant 1/2$ and $-1/2 \leqslant \tilde{q} \leqslant 1/2$ denoted as R:

$$R = \sum_{q,\tilde{q}} \mathrm{Im}[\varepsilon_q(\tilde{q})]. \tag{11}$$

The ratio of R between different lattice depth and $5E_r$ is

$$r(V_0) = \frac{R(V_0)}{R(5E_r)}, \tag{12}$$

which is shown in Fig. 4(d) with the cross points. The solid circles with error bars give the lifetime of oscillation by fitting the experimental data with exponential decay.

As expected, the increasing of V_0 will lead to larger dynamical instability ratio, and lead to the suppression of the oscillation.

VII. CONCLUSION

In conclusion, we demonstrate an effective way of loading atoms directly into the P band using two groups of lattice pulses with different phases to break the parity of the Hamiltonian. Our preparation of the P band with $q = 0$ is different from Ref. [6] where the condensate has a distribution in the regime between $q = -\hbar k$ and $\hbar k$. In our work, the evolution of the condensate in the P- band is studied experimentally. The short-period oscillation due to coherent superposition of different bands and long-period oscillation reflecting the random relative phase between neighboring lattice sites are observed simultaneously. The present experiment paves the way to study the long-time dynamical evolution of the high orbital physics for other novel quantum states, such as fermionic superfluid, molecular condensate, and condensate with special configuration of optical lattice.

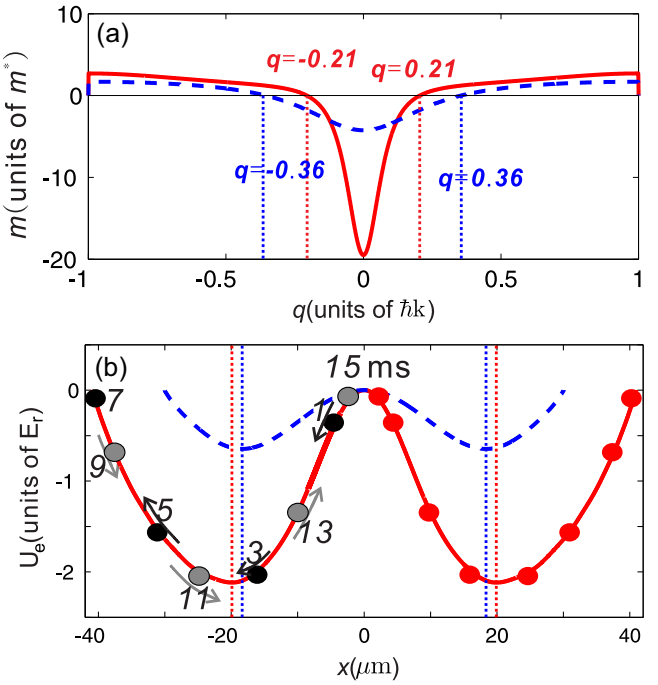

FIG. 5. (Color online) Effective mass for atoms in P band (a) and its effective potential in the presence of a harmonic trap (b) for $5E_r$ (red solid line) and $10E_r$ (blue dashed line). The dotted lines correspond to the points where the sign of the effective mass changes.

ACKNOWLEDGMENTS

This work is partially supported by the state Key Development Program for Basic Research of China under Grant No. 2011CB921501, NSFC (Grants No. 61475007, No. 11334001, and No. 91336103), and RFDP (Grant No. 20120001110091).

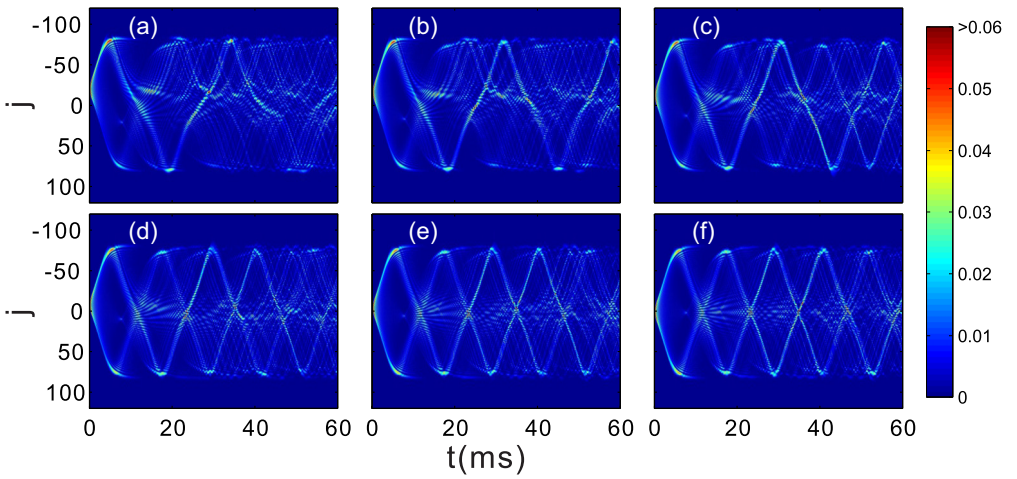

FIG. 6. (Color online) Evolution of different site's wave function for 60 ms with $5E_r$ lattice depth. The simulation includes totally 301 lattice sites. The wave function (a)–(f) is initially distributed in the -25th, -20th, -15th, -10th, -5th, or 0th site, respectively.

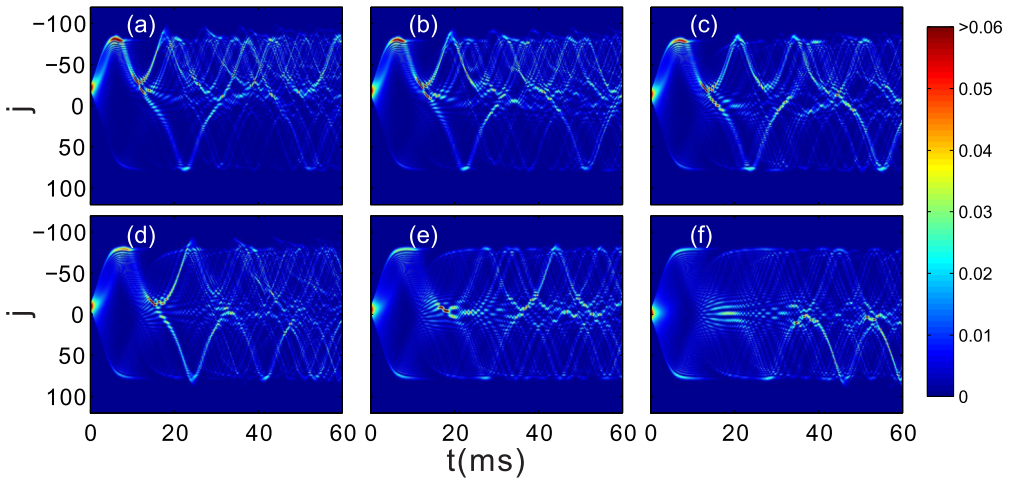

FIG. 7. (Color online) Evolution of different site's wave function for 60 ms with $10E_r$ lattice depth. Other conditions are the same as Fig. 6.

APPENDIX A: EFFECTIVE POTENTIAL MODEL FOR *P*-BAND DYNAMICS

Here we consider a semiclassical model to understand the periodic dynamics in the P band. In the optical lattice, the effective mass is $m^*(q) = \hbar(\partial v/\partial q)^{-1} = \hbar^2(\partial^2 E_p(q)/\partial q^2)^{-1}$, where v is the group velocity and $E_p(q)$ is the energy of the P state for different q. In Fig. 5(a), the ratio between m and m^* is shown for $V_0 = 5E_r$ and $10E_r$, respectively. We see that the effective mass changes sign at the $q = \pm 0.21\hbar k$ and $\pm 0.36\hbar k$ for $V_0 = 5E_r$ and $10E_r$, respectively.

With the semiclassical model, we simplify the problem by considering a quasiparticle with $q = 0$ and study the dynamical process in the harmonic trap. When the effective mass is considered, the acceleration is given as $a(x) = \frac{F(x)}{m^*}$ [32], where $F(x) = -\partial(\frac{1}{2}m\omega^2x^2)/\partial x = -m\omega^2 x$ is the force driven by the harmonic trap without the optical lattice. Using $\frac{dv}{dt} = a$, $\frac{dx}{dt} = v$, $\frac{dq}{dt} = F$, and the initial condition, we get q, m^*, x, and F at time t. Then by expressing all the parameters as a function of x, the dynamical evolution can be described by an effective potential:

$$U_e(x) = -\int_0^x \frac{m}{m^*(x')} F(x')dx'. \tag{A1}$$

In Fig. 5(b), we give the numerical results of the effective potential. This means that the external confinement acts as a repulsive potential [32,33] and the atoms at trap center would be divided into two symmetrical parts for the different momentum states. The minimums of the potential correspond to the points where the sign of the effective mass changes from negative to positive. The initial atoms in the P band at $q = 0$ and $x = \pm 5$ μm near the center of the effective potential would move from the center to the edge (as points denoted by time 1,3,5,7 ms) and then come back (as points by time 9,11,13,15 ms) and form an oscillation.

APPENDIX B: SIMULATION WITH SINGLE-SITE DNLSE

Here we demonstrate the long-period oscillation from the random phase between neighboring lattice sites in detail. As shown before, the simulation without interatomic interaction doesn't have a perfect oscillation. However, when the interference terms between different sites are omitted, we can simulate the evolution of each single site based on the DNLSE [13], and the population n_j would evolute with time as shown in Figs. 6 and 7 for $5E_r$ and $10E_r$ lattice depth, respectively. For $5E_r$, atoms in different lattice sites would be distributed more concentrated during the oscillation, while for $10E_r$ the atoms would disperse more rapidly into different lattice sites.

According to the evolution of the wave function in the jth lattice site $\psi_j(x,t)$ of the optical lattice and the harmonic trap, for each site's evolution, there is a perfect oscillation for the ratio of atoms with momentum $\hbar k$ versus the holding time in the potential. The initial state $\Psi(x,t = 0)$ is the superposition of Wannier functions in different lattice sites. Considering the fact that the randomization between neighboring lattice sites arises from the atomic interaction, the total momentum distribution is given as the weighted incoherent superposition of every site's wave function's evolution. Therefore, the whole atom cloud could also exhibit a good oscillation behavior with time. However, if the coherence term exists, the result would be different, and the collective oscillation is destroyed as shown by the simulation in Fig. 3 of the main body.

[1] P. A. Lee, N. Nagaosa, and X. G. Wen, Rev. Mod. Phys. **78**, 17 (2006).
[2] I. Bloch, J. Dalibard, and W. Zwerger, Rev. Mod. Phys. **83**, 331 (2011).
[3] M. Lewenstein and W. V. Liu, Nat. Phys. **7**, 101 (2011).
[4] T. Sowiński, Phys. Rev. Lett. **108**, 165301 (2012).
[5] T. Sowiński, M. Łącki, O. Dutta, J. Pietraszewicz, P. Sierant, M. Gajda, J. Zakrzewski, and M. Lewenstein, Phys. Rev. Lett. **111**, 215302 (2013).
[6] T. Müller, S. Fölling, A. Widera, and I. Bloch, Phys. Rev. Lett. **99**, 200405 (2007).

[7] V. W. Scarola and S. Das Sarma, Phys. Rev. Lett. **95**, 033003 (2005).
[8] X. Li, Z. Zhang, and W. V. Liu, Phys. Rev. Lett. **108**, 175302 (2012).
[9] W. V. Liu and C. Wu, Phys. Rev. A **74**, 013607 (2006).
[10] C. Wu, Mod. Phys. Lett. B **23**, 1 (2009).
[11] Z. Cai and C. Wu, Phys. Rev. A **84**, 033635 (2011).
[12] F. Pinheiro, G. M. Bruun, J. P. Martikainen, and J. Larson, Phys. Rev. Lett. **111**, 205302 (2013).
[13] F. S. Cataliotti, S. Burger, C. Fort, P. Maddaloni, F. Minardi, A. Trombettoni, A. Smerzi, and M. Inguscio, Science **293**, 843 (2001).
[14] O. Morsch, J. H. Müller, M. Cristiani, D. Ciampini, and E. Arimondo, Phys. Rev. Lett. **87**, 140402 (2001).
[15] A. Trombettoni and A. Smerzi, Phys. Rev. Lett. **86**, 2353 (2001).
[16] Th. Anker, M. Albiez, R. Gati, S. Hunsmann, B. Eiermann, A. Trombettoni, and M. K. Oberthaler, Phys. Rev. Lett. **94**, 020403 (2005).
[17] V. I. Yukalov and E. P. Yukalova, Phys. Rev. A **78**, 063610 (2008).
[18] Y. Y. Zhai, X. G. Yue, Y. J. Wu, X. Z. Chen, P. Zhang, and X. J. Zhou, Phys. Rev. A **87**, 063638 (2013).
[19] X. X. Liu, X. J. Zhou, W. Xiong, T. Vogt, and X. Z. Chen, Phys. Rev. A **83**, 063402 (2011).
[20] X. Chen, A. Ruschhaupt, S. Schmidt, A. delCampo, D. Guéry-Odelin, and J. G. Muga, Phys. Rev. Lett. **104**, 063002 (2010).
[21] S. Masuda, K. Nakamura, and A. delCampo, Phys. Rev. Lett. **113**, 063003 (2014).
[22] A. Browaeys, H. Häffner, C. McKenzie, S. L. Rolston, K. Helmerson, and W. D. Phillips, Phys. Rev. A **72**, 053605 (2005).
[23] P. S. Panahi, D. S. Lühmann, J. Struck, P. Windpassinger, and K. Sengstock, Nat. Phys. **8**, 71 (2012).
[24] C. V. Parker, L. Ha, and C. Chin, Nat. Phys. **9**, 769 (2013).
[25] G. Wirth, M. Ölschläger, and A. Hemmerich, Nat. Phys. **7**, 147 (2011).
[26] D. J. Papoular and S. Stringari, Phys. Rev. Lett. **115**, 025302 (2015).
[27] P. Pedri, L. Pitaevskii, S. Stringari, C. Fort, S. Burger, F. S. Cataliotti, P. Maddaloni, F. Minardi, and M. Inguscio, Phys. Rev. Lett. **87**, 220401 (2001).
[28] M. Gustavsson, E. Haller, M. J. Mark, J. G. Danzl, G. Rojas-Kopeinig, and H. C. Nägerl, Phys. Rev. Lett. **100**, 080404 (2008).
[29] S. Kling, T. Salger, C. Grossert, and M. Weitz, Phys. Rev. Lett. **105**, 215301 (2010).
[30] B. Wu and Q. Niu, Phys. Rev. A **64**, 061603(R) (2001).
[31] B. Wu and Q. Niu, New J. Phys. **5**, 104 (2003).
[32] R. Chang, S. Potnis, R. Ramos, C. Zhuang, M. Hallaji, A. Hayat, F. Duque-Gomez, J. E. Sipe, and A. M. Steinberg, Phys. Rev. Lett. **112**, 170404 (2014).
[33] H. Pu, L. O. Baksmaty, W. Zhang, N. P. Bigelow, and P. Meystre, Phys. Rev. A **67**, 043605 (2003).